Molecular Biology of the Cell
Vol. 19, 3379–3389, August 2008

A Role for Soluble *N*-Ethylmaleimide-sensitive Factor Attachment Protein Receptor Complex Dimerization during Neurosecretion

Elena Fdez,*† Thomas A. Jowitt,†‡ Ming-Chuan Wang,‡ Manisha Rajebhosale,‡ Keith Foster,§ Jordi Bella,‡ Clair Baldock,‡ Philip G. Woodman,‡ and Sabine Hilfiker*

*Institute of Parasitology and Biomedicine "López-Neyra," Consejo Superior de Investigaciones Cientificas, 18100 Granada, Spain; ‡Faculty of Life Sciences, The University of Manchester, Manchester M13 9PT, United Kingdom; and §Syntaxin Ltd., Abingdon, Oxon OX14 3YS, United Kingdom

Submitted January 9, 2008; Revised April 30, 2008; Accepted May 21, 2008
Monitoring Editor: Thomas F. J. Martin

The interactions underlying the cooperativity of soluble *N*-ethylmaleimide-sensitive factor attachment protein receptor (SNARE) complexes during neurotransmission are not known. Here, we provide a molecular characterization of a dimer formed between the cytoplasmic portions of neuronal SNARE complexes. Dimerization generates a two-winged structure in which the C termini of cytosolic SNARE complexes are in apposition, and it involves residues from the vesicle-associated SNARE synaptobrevin 2 that lie close to the cytosol–membrane interface within the full-length protein. Mutation of these residues reduces stability of dimers formed between SNARE complexes, without affecting the stability of each individual SNARE complex. These mutations also cause a corresponding decrease in the ability of botulinum toxin-resistant synaptobrevin 2 to rescue regulated exocytosis in toxin-treated neuroendocrine cells. Moreover, such synaptobrevin 2 mutants give rise to a dominant-negative inhibition of exocytosis. These data are consistent with an important role for SNARE complex dimers in neurosecretion.

INTRODUCTION

Neurotransmitter release occurs when synaptic vesicles fuse with the plasma membrane. A crucial step in this process involves the assembly of a soluble *N*-ethylmaleimide-sensitive factor attachment protein receptor (SNARE) complex, a highly stable, parallel four-helix bundle formed between the synaptic vesicle SNARE synaptobrevin 2 (syb2) and the plasma membrane SNAREs syntaxin 1 and synaptosome-associated protein of 25 kDa (SNAP-25) (Söllner *et al*., 1993; Hanson *et al*., 1997; Sutton *et al*., 1998; Südhof, 2004; Jahn and Scheller, 2006; Rizo *et al*., 2006; Wojcik and Brose, 2007). Current data suggest that SNARE complex formation proceeds in a vectorial manner from the N-terminal, membrane-distal region toward the C-terminal, membrane-proximal end, which may draw the opposing membranes close enough together for fusion to proceed (Fiebig *et al*., 1999; Pobbati *et al*., 2006; Sorensen *et al*., 2006). Consistent with this, in reconstituted assay systems, SNAREs on their own can support membrane fusion (Weber *et al*., 1998; Hu *et al*., 2003; Giraudo *et al*., 2006; Pobbati *et al*., 2006).

In intact cells, evoked membrane fusion involves the cooperative action of multiple SNARE complexes (Cull-Candy *et al*., 1976; Bevan and Wendon, 1984; Stewart *et al*., 2000). The exact number of complexes required is currently unknown, and estimates vary from three (Hua and Scheller, 2001) to five to eight (Han *et al*., 2004) to 10–15 (Keller and Neale, 2001; Keller *et al*., 2004; Montecucco *et al*., 2005). Such differences may reflect the distinct experimental paradigms used and/or the types of secretory organelles studied. Thus, higher order multimers of SNARE complexes may be required for fast exocytosis of synaptic vesicles, whereas lower order multimers may be sufficient for the slower exocytosis of large dense-core granules from chromaffin and neuroendocrine PC12 cells (Montecucco *et al*., 2005).

The mechanism(s) responsible for SNARE complex multimerization remains controversial. Initial studies suggested that multimerization of synaptic SNARE complexes could be achieved via domain swapping, whereby one of the two SNAP-25 helices could be substituted by the equivalent helix from a neighboring complex (Kweon *et al*., 2002). Alternative models proposed the involvement of accessory proteins, such as synaptotagmin (Littleton *et al*., 2001) or complexin (Tokumaru *et al*., 2001), or the transmembrane domains of syb2 and syntaxin 1A (Laage *et al*., 2000), in synaptic SNARE complex multimerization. However, SNARE complexes assembled from recombinant coils and lacking transmembrane domains are able to associate with each other (Fasshauer *et al*., 1997; Fasshauer *et al*., 1998; Margittai *et al*., 2001; Ernst and Brünger, 2003), arguing that at least some of the interactions that support multimerization may require neither

This article was published online ahead of print in *MBC in Press* (http://www.molbiolcell.org/cgi/doi/10.1091/mbc.E08–01–0010) on May 28, 2008.

† These authors contributed equally to this work.

Address correspondence to: Sabine Hilfiker (sabine.hilfiker@ipb.csic.es).

Abbreviations used: MALLS, multiangle laser light scattering; SAXS, small angle X-ray scattering; SNARE, soluble *N*-ethylmaleimide-sensitive factor attachment protein receptor; syb2, synaptobrevin 2; TEM, transmission electron microscopy.

accessory proteins nor transmembrane domains. The precise multimeric nature and configuration of these recombinant cytosolic SNARE complexes is ambiguous. Conflicting results have been reported, ranging from dimers involving C-terminal residues of at least one of the two monomers, to mixtures of monomers/trimers in solution (Fasshauer *et al*., 1997, 1998; Margittai *et al*., 2001; Ernst and Brünger, 2003). In addition, no investigations have addressed whether such interactions between SNARE complexes might contribute to their biological action.

To test whether multimerization of SNARE complexes mediated by their cytosolic domains is an important step during neurotransmitter release, we first performed a detailed characterization of how such multimers are configured. We identified amino acids within synaptobrevin 2 that contribute to a cytosolic SNARE complex dimer formed with micromolar affinity. Functional analysis of synaptobrevin 2 mutants in which these residues are replaced provides evidence for an important role for SNARE complex dimers during exocytosis.

MATERIALS AND METHODS

Plasmids and Protein Purification

Constructs encoding sequences for the "coils" that form the "minimal" SNARE complex of rat syntaxin 1a (191-262), synaptobrevin 2 (syb2) (1-96), SNAP-25 B (1-83), and SNAP-25 B (120-206), constructs encoding full-length nontagged syb2 and green fluorescent protein (GFP)-tagged syb2 and fluorescence resonance energy transfer (FRET) probes were generated using standard polymerase chain reaction (PCR) and cloning procedures (for details see Supplemental Material). Recombinant proteins were expressed as N-terminally tagged glutathione S-transferase (GST) fusion proteins and purified using standard protocols (Söllner *et al*., 1993; also see Supplemental Material). Protein concentrations were estimated by the Bradford assay, and they ranged from 0.3 to 1 mg/ml. SNARE complexes were formed by overnight assembly of equimolar concentrations of purified components in standard buffer and concentrated to ~2 mg/ml. Complex formation was verified by SDS-polyacrylamide gel electrophoresis (PAGE). Determination of synaptotagmin 1 and complexin binding to SNARE complexes was performed as described in Supplemental Material.

Multiangle Laser Light Scattering (MALLS)

SNARE complexes were purified from recombinant coils on a Superdex-200 24/30 gel filtration column (GE Healthcare, Chalfont St. Giles, United Kingdom) run in 5 mM Tris-HCl, pH 7.4, 50 mM NaCl at 0.71 ml/min using a BioLC high-performance liquid chromatography (Dionex, Camberley, United Kingdom). The SNARE complex dimer peak resolved clearly from the mixture. For SNARE complex mutants all molecular weight (MW) analysis refers to that of material within the dimer peak, although some SNARE complex monomer could also be found (data not shown). Protein passed through a Wyatt EOS 18-angle laser photometer (Wyatt Technology, Santa Barbara, CA) with the 13th detector replaced with a QELS detector (Wyatt Technology) for the simultaneous measurement of hydrodynamic radius. This was coupled to an Optilab rEX refractive index detector (Wyatt Technology), and the hydrodynamic radius, molecular weight moments, and concentration of peaks were analyzed using Astra 4.98 (Wyatt Technology).

Analytical Ultracentrifugation

SNARE complex dimers (~8 μM) were purified by gel filtration. All experiments were performed in 5 mM Tris-HCl, pH 7.4, containing the indicated concentrations of NaCl, and using a XL-A ultracentrifuge (Beckman Coulter, Fullerton, CA) with an An50Ti 8-hole rotor fitted either with the standard two-sector open-filled centerpieces for sedimentation velocity, or with six-sector Epon-filled centerpieces for equilibrium studies, with quartz glass windows. Velocity sedimentation analysis was performed at 40,000 rpm at 20°C, with the sedimenting boundary monitored at 230 nm every 9 min. Frictional ratios for the monomer and dimer were calculated from the sedimentation coefficient. For data interpretation and solution bead modeling, see Supplemental Material.

Equilibrium sedimentation was performed at 4°C, using rotor speeds of 10, 15, and 21,000 rpm and scanning at 230 nm every 4 h until equilibrium was reached. For molecular weight analysis, data were analyzed with the fitting program HeteroAnalysis by using a single ideal model for a distribution of the mean molecular weight. Data were expressed as the average MW from this approximation (MW_{app}) relative to the theoretical MW of the monomer. Association constants were investigated using concentrations of 1, 2.5, and 5 μM protein at the same three rotor speeds in 5 mM Tris-HCl and 0.3 M NaCl. Global analysis using Sedphat (developed by Peter Schuck, National Institutes of Health, Bethesda, MA) of a monomer–dimer association produced the best fit.

Small Angle X-Ray Scattering Data Collection

Small angle X-ray solution scattering (SAXS) was carried out using gel filtration-purified SNARE complex dimers (8 μM) on ID02 at the European Synchrotron Radiation Facility (Grenoble, France) by using 1-m and 5-m sample to detector distances. During data collection, the sample was maintained at 10°C. The corresponding profiles were merged so as to cover the momentum transfer interval $0.0038\ \text{Å}^{-1} < q < 0.53\text{Å}^{-1}$. The modulus of the momentum transfer is defined as $q = 4\pi\sin\theta/\lambda$, where 2θ is the scattering angle, and λ is the wavelength. With a 1-m camera distance the maximum scattering angle corresponds to a Bragg resolution of 11.8 Å. SAXS patterns were recorded using an image intensified charge-coupled device (CCD) detector having single photon sensitivity and 14 bit dynamic range. The wavelength of X-rays used was 0.1 nm. For further details about data collection and analysis, see Supplemental Material.

Transmission Electron Microscopy (TEM) Single Particle Image Analysis

Gel filtration-purified SNARE complex dimers were concentrated threefold (24 μM), and 5 μl of sample was allowed to adsorb for 30 s onto a glow discharged (25 mA for 30 s) carbon-coated 400 mesh copper grid. The grid was washed three times with MilliQ water (Millipore, Billerica, MA) and then negatively stained with 2% (wt/vol) uranyl acetate, pH 4.7, for 20 s. Grids were observed using a Tecnai Twin TEM (FEI, Hillsboro, OR) equipped with a LaB_6 filament operating at 120 keV. Images were recorded under low dose conditions at −600-nm defocus on a 2048 × 2048 CCD camera with a pixel size of 2 Å. The level of defocus of each individual image was checked by inspecting the position of the Thon rings in the power spectra and comparing this to the calculated contrast transfer function. For details on image processing, see Supplemental Materials.

Fluorescence Spectroscopy

SNARE complexes (~5 μM) were purified by gel filtration chromatography, and tryptophan fluorescence was measured in a 100-μl, 1-cm path-length cell using an FP750 spectrofluorometer (Jasco, Tokyo, Japan) by excitation at 295 nm and monitoring of emission fluorescence between 300 and 450 nm.

CD Spectroscopy

The CD spectra of SNARE complexes (2–5 μM) purified by gel filtration chromatography were monitored from 260 to 190 nm in 0.2-nm steps (with 10 averages assayed) in a 0.05-cm pathlength cuvette by using a J810 spectropolarimeter (Jasco).

Differential Scanning Calorimetry

The stability of SNARE complexes was investigated using a VP-DSC microcalorimeter (MicroCal, Northampton, MA) with a 0.52-ml total loading volume (also see Supplemental Materials).

FRET Measurements

GFP-tagged SNARE complexes (see Supplemental Materials for details) were purified by gel filtration chromatography (4 μM), and molecular mass was analyzed by MALLS as described above, with a determined mass of 144 ± 4 kDa, close to the predicted mass of 146 kDa for GFP-tagged SNARE complex dimers. Purified C-C– or N-C–tagged SNARE complex dimers were analyzed using a J750 spectrometer (Jasco) and a 100-μl, 1-cm pathlength cell. The excitation wavelength was 433 nm, and emission spectra were measured between 450 and 650 nm in 1-nm steps.

Determination of Localization and Expression Levels of syb2 and of SDS-resistant SNARE Complex Stability

The overexpression levels of nontagged syb2 and mutants thereof, the localization of GFP-tagged syb2 and mutants thereof, and the determination of GFP-tagged SDS-resistant SNARE complex stabilities, were determined as described in Supplemental Material.

Secretion Assays

Confluent PC12 cells were plated onto collagen-coated six-well dishes at 80% confluence, and then they were transfected the following day with 3 μg of DNA by using 10 μl of Lipofectamine 2000 (Invitrogen, Paisley, United Kingdom). Cells were replated into six-well dishes at a ratio of 1:2 the next day, and secretion assays performed two days after replating, with all test and control conditions carried out on the same pool of transfected cells. Controls were treated with 0.6 ml of physiological saline solution (PSS; 145 mM NaCl, 5.6 mM KCl, 2.2 mM $CaCl_2$, 0.5 mM $MgCl_2$, 5.6 mM glucose, and 15 mM HEPES-NaOH, pH 7.4), and evoked neurosecretion was triggered by a 5-min

Table 1. Comparison of experimentally derived and modelled hydrodynamic data for monomeric and dimeric SNARE complexes

A

		Experimental hydrodynamic results			
	MW[a]	$S^0_{20,W}$	f/f_0	R_H[b]	R_H[c]
WT monomer	44,600	3.05 ± 0.148	1.49	3.23 ± 0.25	N.D.
WT dimer	89,500	4.13 ± 0.135	1.75	5.02 ± 0.10	4.9

N.D., not determined.
[a] Molecular weight derived from light scattering.
[b] Hydrodynamic radius from analytical ultracentrifugation (AUC).
[c] Hydrodynamic radius from light scattering.

B

	Bead model hydrodynamics					
	Monomer	Dimer: 90°	120°	130°	140°	180°
R_H (nm)	3.22	4.63	4.82	4.91	5.10	5.20
$S^0_{20,W}$	3.26	4.58	4.40	4.32	4.16	4.08

(A) Hydrodynamic information for SNARE complex monomers and dimers was determined experimentally, by using MALLS or AUC as indicated. Predicted molecular weight for a monomeric SNARE complex, including vector-derived amino acids, is 45,768 Da. (B) Solution bead models of the SNARE complex monomer were generated using atomic coordinates of SNARE coiled-coil domains and the solution modelling software SOMO. End-end dimers, in which the monomers were oriented at the indicated angles with respect to each other, were generated using PyMOL (http://pymol.sourceforge.net/). Hydrodynamic parameters were generated for the monomer and for all dimer models. Note that the bead model of the SNARE complex monomer generated very similar hydrodynamic values to those observed experimentally, indicating a high level of confidence for the modelling. Comparison with the experimentally determined hydrodynamic parameters shows that the closest fit for the dimer is achieved with an end-to-end dimer oriented at ~130–140°.

incubation with high K^+ saline solution (PSS containing 95 mM NaCl and 56 mM KCl). The amount of human growth hormone (hGH) in the medium and in cells was determined by an enzyme-linked immunosorbent assay, and the total amount of hGH and the percentage hGH secreted calculated against an hGH standard curve. Statistical analyses were performed with the paired Student's *t* test.

Toxin Rescue Assays

Release of hGH from toxin-treated, permeabilized PC12 cells transfected with botulinum neurotoxin type B (botB)-resistant syb2 (Q76V,F77W) was measured essentially as described previously (Quetglas *et al.*, 2002) in the presence of recombinantly expressed endopeptidase light chain (LC) of botB (botB/LC). BotB/LC was purified as described previously (Sutton *et al.*, 2005), was of high homogeneity as assessed by SDS-PAGE, and it showed endopeptidase activity comparable with native botulinum neurotoxin by using an in vitro vesicle-associated membrane protein peptide cleavage assay (Sutton *et al.*, 2005). Determination of the cleavage of endogenous syb2 upon toxin treatment, and of the levels of expressed toxin-insensitive syb2 and syb2 mutants, are described in Supplemental Material.

RESULTS

Global Solution Structure of Synaptic SNARE Complex Multimers

As an essential step toward testing whether multimerization of SNARE complexes facilitated by interactions between their cytosolic domains is important for neurotransmitter release, we first ascertained whether cytosolic portions of SNARE complexes would form multimers of defined stoichiometry and configuration in solution. SNARE complexes encompassing the cytoplasmic coiled coil-forming motifs of syb2, syntaxin 1, and SNAP-25 (Supplemental Figure 1) were purified by size exclusion chromatography to yield a single major peak containing assembled SNAREs (Supplemental Figure 2A; data not shown). When rechromatographed and analyzed by MALLS, they yielded a molecular weight of 89,500 Da (Supplemental Figure 2B and Table 1A), twice that of a monomeric SNARE complex. Treatment with 1 M NaCl (Antonin *et al.*, 2000) reduced the molecular weight to 44,600 Da (Supplemental Figure 2B). Hence, cytosolic neuronal SNARE complexes are quantitatively incorporated into salt-sensitive dimers.

To explore how this dimer is configured, we first examined its shape in solution. Initially, purified SNARE complexes were subjected to velocity sedimentation in low or high salt. Surprisingly, the sedimentation coefficients of the dimer and monomer were relatively close, whereas the frictional ratio was appreciably different and the hydrodynamic radius of the dimer was much larger than that of the monomer (Figure 1A and Table 1A). These data suggest that the dimer is more elongated than the monomer, and they argue against it forming by extensive alignment of monomers.

The solution shape of the dimer was determined more precisely by using small angle X-ray solution scattering (SAXS). The experimental scattering profiles were modeled using an ab initio procedure (Svergun, 1999; Svergun *et al.*, 2001) (Supplemental Figure 3), and the averaged filtered structure resolved as a two-winged particle with each wing ~9.5 nm long and tilted at ~110° relative to each other (Figure 1B). Using transmission electron microscopy to determine the shape directly revealed a similar structure, with each wing 9–10 nm long and set at 140° to each other (Figure 1C).

To confirm that these shapes are consistent with the observed hydrodynamic properties, bead models were generated from the atomic coordinates within SNARE complexes (Sutton *et al.*, 1998) by using the program SOMO (Spotorno *et al.*, 1997), and then they were aligned in hypothetical

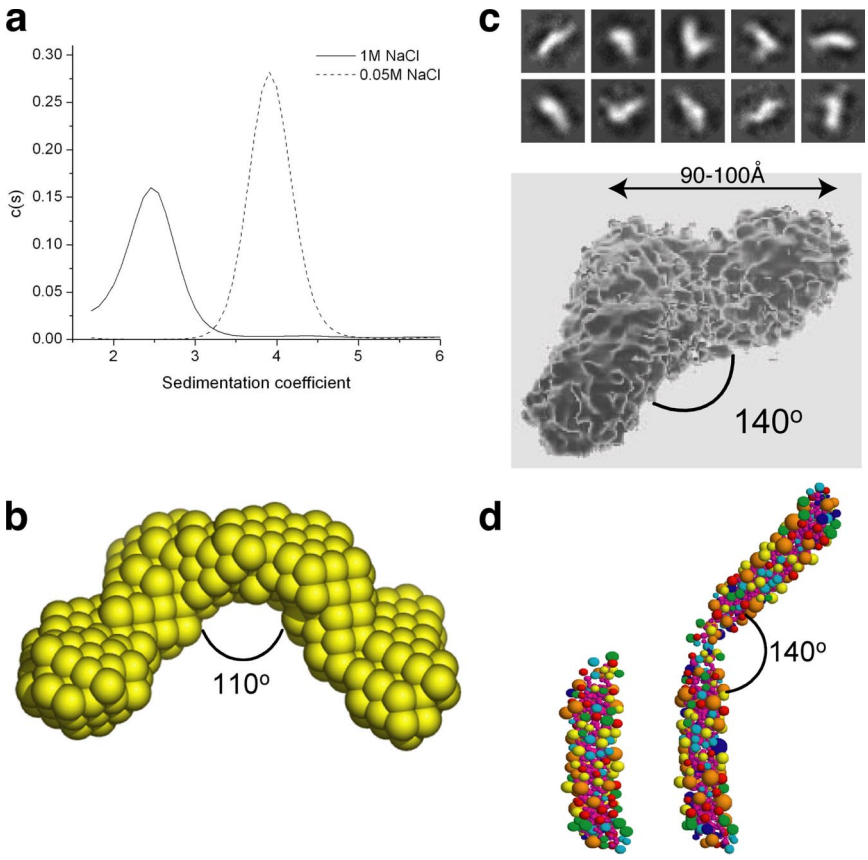

Figure 1. Neuronal SNARE complexes form a wing-shaped, end-to-end dimer. Purified SNARE complex dimers were analyzed by sedimentation in 50 mM (dashed line) or 1 M (solid line) NaCl (a); SAXS, with shapes simulated ab initio and the "most probable" shape represented as an arrays of beads (b); TEM, with the 10 most common shape classes shown above and an average refined structure below (c); and aligning SNARE complex monomer bead models (left) to generate a shape matching the observed hydrodynamic properties (right) (d).

configurations and modeled for their hydrodynamic properties. End-to-end dimers set at an angle of 130–140° generated hydrodynamic properties close to those observed experimentally (Figure 1D and Table 1B). Thus, three methods of shape analysis suggest that cytosolic SNARE complexes form uniformly configured dimers, in which the dimerization interface lies close to one end of each SNARE complex and generates an open, two-winged structure.

Orientation of the SNARE Complex Dimer

Fusion of primed vesicles requires conversion of partially assembled *trans*-SNARE complexes into fully assembled, fusion-competent SNARE bundles (Fiebig *et al*., 1999; Pobbati *et al*., 2006; Sorensen *et al*., 2006). Therefore, a functionally relevant dimer should involve C-terminal SNARE complex regions that lie close to the point of membrane insertion. To address whether the C termini of SNARE complexes are close to each other within a dimer, we measured FRET in SNARE complexes assembled using a mixture of syb2-cyan fluorescent protein (CFP) and syb2-Venus, providing complexes containing either FRET donor or FRET acceptor at the C terminus (Figure 2A). For comparison, SNARE complexes were assembled using syb2-Venus and CFP-syb2. All complexes formed with similar efficiency, and they were equally stable, compared with those containing wild-type (wt) syb2 (data not shown; Supplemental Figure 4). However, only when both FRET partners were located at the C termini of syb2 molecules was a significant FRET signal observed that was sensitive to disruption of the dimer by high salt (Figure 2, B and C). Hence, the C termini of both individual, soluble SNARE complex monomers are adjacent to each other in the dimer. This would suggest that dimers could form in vivo only when SNARE complex assembly is virtually complete.

Residues Involved in Forming the Dimer Interface

To test the functional significance of this dimer, we first identified amino acids that contribute to dimerization. We focused initially on neighboring tryptophan residues (W89 and W90) within syb2 that are adjacent to the cytosol–membrane interface and hence likely to be close to the point of dimerization (Figure 3A). Because these are the only tryptophans within the cytosolic SNARE complex, any changes in intrinsic tryptophan fluorescence upon conversion of dimers to monomers would indicate that these residues form part of the dimer interface. Indeed, the tryptophan fluorescence decreased with increasing [NaCl] (Figure 3B), closely matching the monomerization of SNARE complex dimers determined independently by equilibrium sedimentation (Figure 3C). The peak fluorescence emission wavelength remained unchanged (~355 nm) at all [NaCl] (Figure 3B, inset), suggesting that the tryptophan residues in both SNARE complex dimers and monomers occupy hydrophilic environments. Thus, the fluorescence decrease upon monomerization most likely results from release of rotational constraints imposed upon at least one tryptophan residue within the dimer and suggests that one or both tryptophans participate in dimerization.

Mutational analysis provided direct evidence for this. Equilibrium sedimentation of SNARE complex dimers containing syb2(W89A,W90A) showed that they were more sensitive to increasing [NaCl] than wild-type dimers (Figure 3C and Table 2A). Analysis of single mutants revealed that dimers containing syb2(W89A) displayed NaCl sensitivity

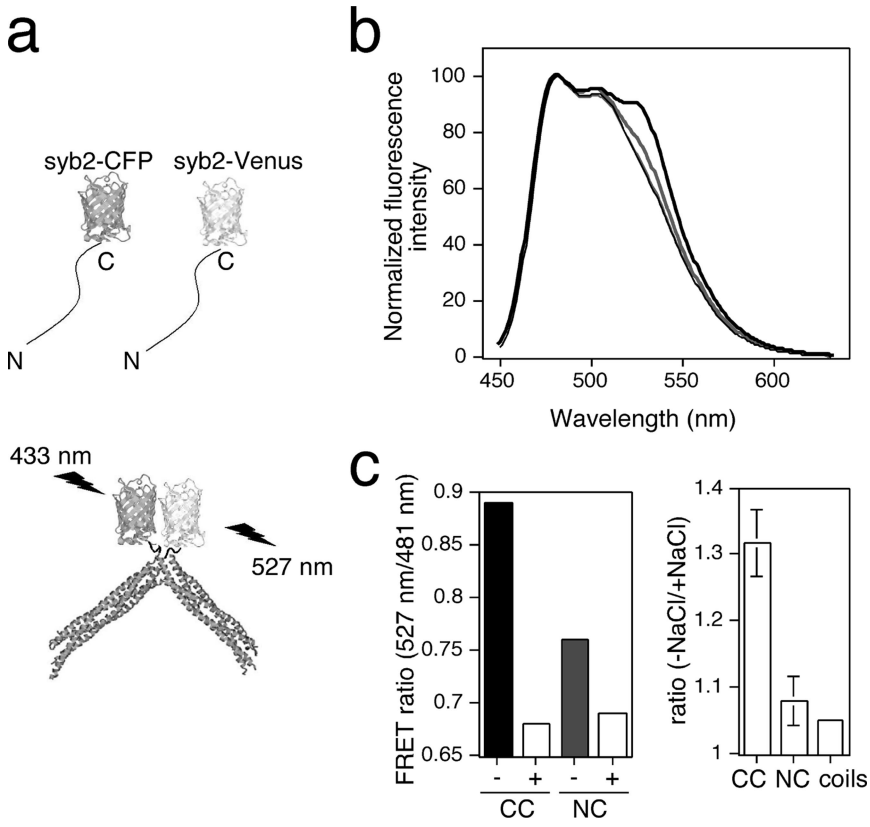

Figure 2. The C termini of both SNARE complex monomers are adjacent to each other in the dimer. (a) Schematic diagram of C-terminally tagged FRET syb2 proteins, uncomplexed or incorporated into SNARE complex dimers. (b) Emission spectra of purified dimers tagged at the C terminus with Venus as FRET acceptor, and either at the C terminus (black) or N terminus (gray) with CFP as FRET donor. Spectra are shown in the absence (thick lines) or presence (thin lines) of 1 M NaCl, and were normalized to their values at 481 nm (CFP emission peak). (c) Left, FRET ratios (emission ratio 527/481 nm) from experiments depicted in b, where − and + refer to the absence or presence of 1 M NaCl, respectively. Right, ratio of FRET ratios (−NaCl/+NaCl) obtained with SNARE complex dimers tagged at both C termini (CC) or at the C terminus and N terminus (NC), or obtained with tagged syb2 proteins only (coils). Values are mean ± SEM (n = 5).

similar to those containing syb2(W89A,W90A), whereas those containing syb2(W90A) were slightly more stable than wild type (Figure 4A). Hence, W89 makes the greater contribution to dimer stability. However, both tryptophans seem to lie at the dimer interface, as the tryptophan fluorescence from W90 in SNARE complex dimers formed using syb2(W89A) decreased in intensity at NaCl concentrations that caused dimer disassembly (Figure 4B). This would indicate that it is W90 that is subject to rotational constraints within the dimer.

We reasoned that residues close to W89-W90 may also contribute to the dimer interface. To this end, we tested effects of mutating the conserved residue R86 within syb2 on dimer stability. Indeed, dimers formed using syb2(R86A), and syb2(R86A,W89A,W90A) were substantially more sensitive to increased [NaCl] (Figure 3C and Table 2A). To compare affinities using sedimentation analysis, SNARE complexes were analyzed after dilution in 0.3 M NaCl, a salt concentration at which wild-type and mutant SNARE complexes are all at equilibrium between monomers and dimers (Figure 3C). The association constant for each SNARE dimer species was obtained by global analysis of concentration-dependent dimerization at equilibrium (Supplemental Figure 5). The association constant was 5.43 μM for wild-type SNARE complex dimers, compared with 11.97 and 46.23 μM for those containing syb2(W89A,W90A) and syb2(R86A,W89A, W90A), respectively. Analysis of sedimentation experiments performed using wild-type SNARE dimers at varying salt concentrations confirmed that the association constant was linear with respect to [NaCl] (data not shown), yielding an estimated association constant of 1.23 μM at 150 mM NaCl, close to physiological ionic strength.

The mutations that we have identified substantially reduce the affinity of SNARE complex dimerization. Importantly, however, they do not affect the stability of each SNARE complex monomer significantly. These formed with identical helicity to wild-type SNARE complexes, assessed by the CD spectroscopy peak at 220 nm (Figure 3D). Differential scanning calorimetry was used to provide a precise estimate of the energy associated with SNARE complex formation and showed that the very high stability of the SNARE complex coiled-coil helix was essentially unaffected by the syb2 dimerization mutations; the melting temperature for all SNARE complexes was very similar and the change in enthalpy associated with this transition was not altered significantly (Figure 3E and Table 2B). Incorporation of syb2(R86A) displayed a slight effect on the stability of individual SNARE complexes (Figure 3E), but importantly, this was not observed when syb2(R86A,W89A,W90A) was used. In summary, our data indicate that three residues of syb2 (R86, W89, and W90) form part of the interaction interface of an open, wing-shaped SNARE complex dimer as observed in solution. In addition, because the two tryptophan residues are fully solvent exposed, the salt sensitivity of the dimer is likely due to salt-dependent changes in its structure, including disruption of salt bridge(s) involving R86.

Syb2 Dimerization Mutants Are Unable to Support Secretion

We next aimed to determine whether residues in syb2 found at the SNARE complex dimer interface in vitro may be important for supporting neurosecretion in vivo. For this purpose, we transfected neuroendocrine PC12 cells with a plasmid containing both syb2 and hGH (Sugita *et al.*, 1999). Cells were then permeabilized and treated with recombinant botulinum neurotoxin type B light-chain (botB/LC) (Sutton *et al.*, 2005), which cleaves and inactivates syb2 (Figure 5A).

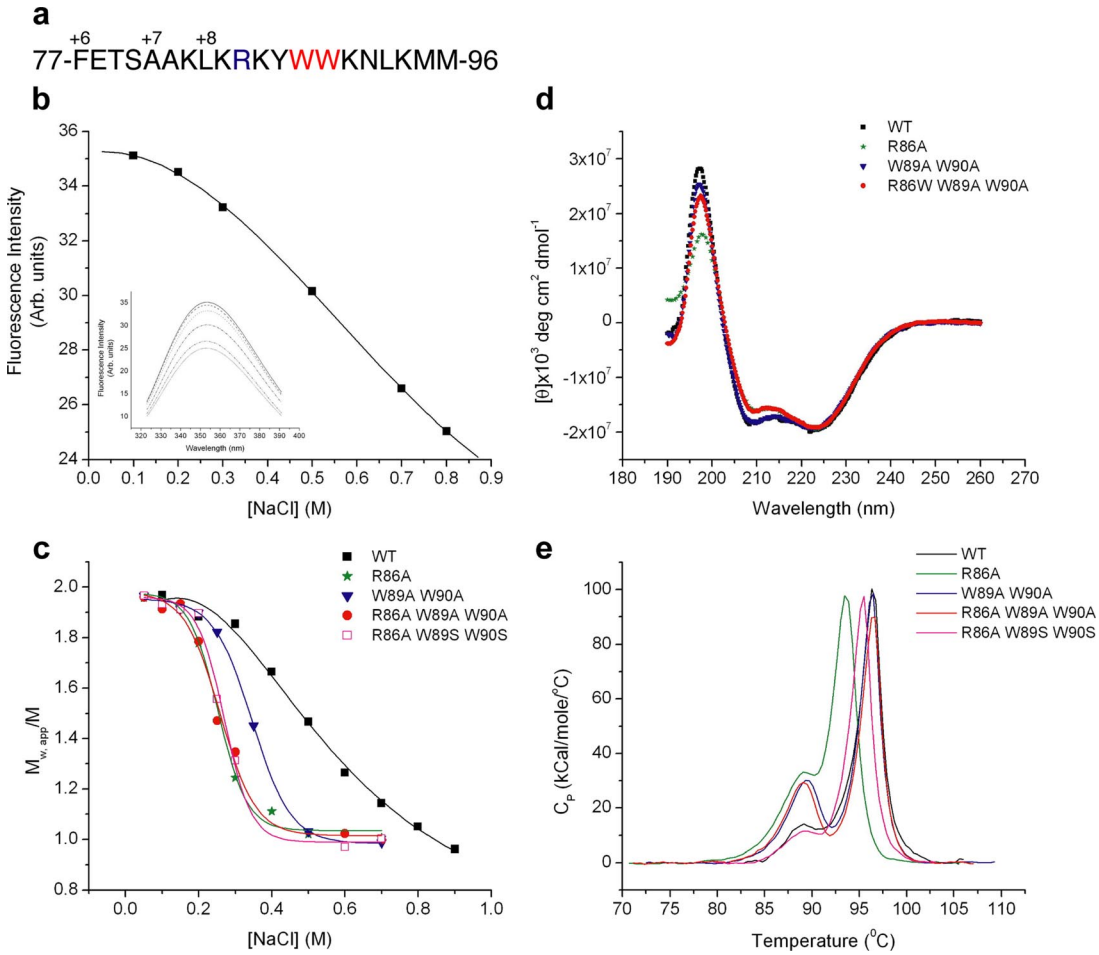

Figure 3. Three residues from syb2 form part of the dimer interface. (a) Sequence of membrane-proximal region of syb2, with amino acids important for SNARE complex dimer stability colored and the position of hydrophobic SNARE motif layers indicated above. (b) Peak intrinsic fluorescence of SNARE complex dimers at increasing [NaCl] (inset, full emission spectra). Fluorescence intensity of free tryptophan remains unchanged with increasing [NaCl] (data not shown). (c) Dimers containing wild-type (black); W89A,W90A (blue); R86A (green); R86A,W89A,W90A (red); and R86A,W89S,W90S (magenta) syb2 were measured for their sensitivity to [NaCl] by using sedimentation equilibrium. (d) α-Helical content using CD spectroscopy (R86A,W89S,W90S mutant not determined). (e) SNARE complex melting temperature using differential scanning calorimetry.

As expected, Ca^{2+}-dependent secretion of hGH was decreased (to 32% of control) by the presence of botB/LC in cells transfected with a plasmid containing wild-type syb2 (Figure 5B). Such profound, but incomplete inhibition of release has been described previously (Chilcote *et al*., 1995; Quetglas *et al*., 2002). The expression of botB/LC-resistant syb2(Q76V,F77W) restored secretion (104% of control) in the presence of toxin (Figure 5B). This rescue assay allowed us to measure the ability of syb2 dimerization mutants to support exocytosis in the absence of endogenous protein. Toxin-insensitive wild-type and mutant syb2 were all expressed to similar degrees (Figure 5C). However, toxin-insensitive syb2(W89A,W90A) was severely impaired in its ability to rescue secretion (17.5% of control) (Figure 5D), similar to what has been described previously (Quetglas *et al*., 2002). Using this assay system, no further additive effects could be observed using syb2(R86A,W89A,W90A), which was equally deficient in supporting release. Interestingly, syb2(W90A) displayed a slight deficit in its ability to rescue secretion, with syb2(W89A) displaying more pronounced effects (Figure 5D). Hence, the ability of syb2 mutants to support release in vivo reflects the contribution of each corresponding amino acid to the SNARE complex dimer interface. Previous studies have implicated W90 in calmodulin-dependent regulation of exocytosis (Quetglas *et al*., 2000, 2002). However, because W90A would disrupt the calmodulin binding motif within syb2 (Rhoads and Friedberg, 1997; Chin and Means, 2000), the ability of this mutant to largely support secretion would suggest that such an interaction does not play a major role in vivo.

Dominant-Negative Secretory Effects of Syb2 Dimerization Mutants

To further test the importance of SNARE complex dimers during regulated exocytosis, we used a dominant-negative approach. Because PC12 cells display Ca^{2+}-evoked secretion that requires cooperativity between three or more SNARE complexes (Hua and Scheller, 2001), expression of full-length syb2 mutants that are incorporated into SNARE complexes of normal stability but impaired in dimer formation should generate a dominant-negative phenotype, revealing a potential role for SNARE complex dimerization in membrane fusion.

Table 2. Syb2 mutants reduce stability of SNARE complex dimers but not monomers

A

Syb2 in complex	Molecular wt (Da) MALLS (errors from polydispersity)	Molecular wt (Da) Sedimentation equilibrium (SD, n = 3)	Hydrodynamic radius (nm) (MALLS)	NaCl conc. 50% monomer
WT	91,630 ± 916	82,546 ± 314	5.1 ± 0.2	0.52 ± 0.017
W89AW90A	92,120 ± 644	84,289 ± 991	4.8 ± 0.3	0.37 ± 0.008
R86A-W89AW90A	89,910 ± 225	84,554 ± 1978	4.8 ± 0.3	0.26 ± 0.016
R86A-W89SW90S	88,900 ± 800	85,167 ± 1207	4.9 ± 0.2	0.27 ± 0.01

B

Syb2 in complex	T_m (°C)	ΔH (kCal mol^{-1})	ΔH_{VH} (kCal mol^{-1})
WT	96.20 ± 0.04	286 ± 7.4	340 ± 10.9
W89AW90A	96.15 ± 0.02	276 ± 4.0	369 ± 7.9
R86A-W89AW90A	96.22 ± 0.02	265 ± 4.0	355 ± 7.1
R86A-W89SW90S	95.17 ± 0.03	286 ± 6.8	346 ± 10.0

(A) Dimer stability: wild-type and syb2 mutant SNARE complexes were purified by size exclusion and analyzed by MALLS or analytical ultracentrifugation. [NaCl] at which SNARE complexes are 50% monomeric is taken from Figure 4c. (B) Monomer stability: SNARE complexes were subjected to differential scanning calorimetry to obtain melting point temperatures (Figure 3e). ΔH is based on integration of the melting point transition, whereas ΔH_{VH} is based on peak width and is independent of protein concentration.

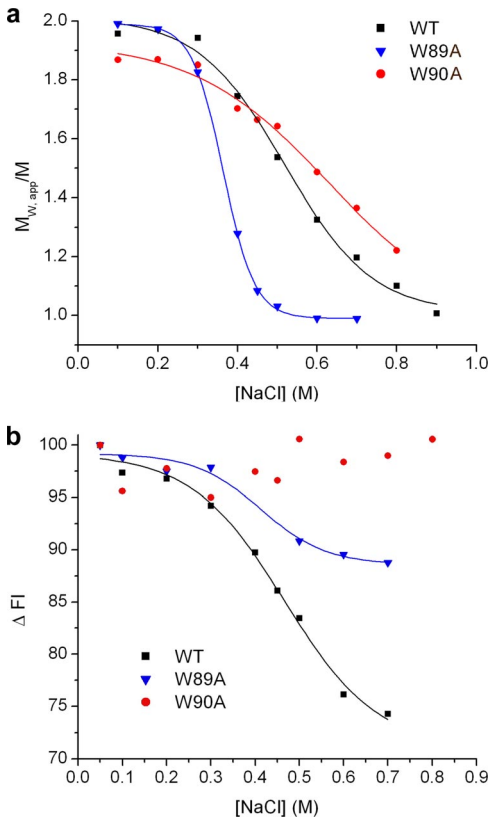

Figure 4. Relative contribution of individual tryptophan residues within syb2 to dimer interface. (a) Dimers containing wild-type (black), W89A (blue), and W90A (red) syb2 were measured for their sensitivity to [NaCl] by using sedimentation equilibrium. (b) Peak intrinsic fluorescence of SNARE complex dimers containing wild-type (black), W89A (blue), and W90A (red) syb2 at increasing [NaCl]. Fluorescence intensity is expressed relative to the emission maximum of each protein complex in 50 mM NaCl.

PC12 cells were transfected with syb2 and hGH as described above, and intact cells were assayed directly to measure constitutive and evoked exocytosis. Exogenous syb2 was expressed at ~2–3 times over endogenous levels, and all mutants analyzed were expressed to similar degrees (Figure 6A). Expression of wild-type syb2 did not affect basal or evoked secretion of hGH (data not shown). In contrast, expression of syb2 dimerization mutants reduced evoked secretion without affecting basal secretion or levels of hGH expression (Figure 6B). This inhibition was reproducible, statistically significant, and greatest for syb2(R86A,W89A, W90A), in line with the more pronounced effect of this mutant on SNARE complex dimer stability (Figure 6C). All syb2 constructs analyzed in this study localized to neuritic appendages and were efficiently incorporated with endogenous SNARE proteins into SNARE complex monomers of essentially the same stability, assessed by heating in SDS (Figure 6, E–H, and Supplemental Figures 6 and 7).

Complexins and synaptotagmin 1 bind to SNARE complexes with distinct outcomes for membrane fusion reactions (Tang *et al.*, 2006). Because such interactions may be mutually exclusive with SNARE complex dimerization, we formed SNARE complexes in the presence of complexin 1 or synaptotagmin 1, respectively, and we measured the extent of dimer formation by size exclusion chromatography. SNARE complex dimerization was not prevented by an excess of complexin 1, which coeluted with SNARE complex dimers (Supplemental Figure 8, A and B). Binding was essentially stoichiometric, as judged by the substantial change in apparent molecular weight of dimeric SNARE complexes in the presence of complexin 1. Complexin 1 bound to wild-type and syb2(R86A,W89A,W90A)-containing SNARE complexes with similar efficiency, consistent with complexin binding to a site within the SNARE complex distinct from the dimerization interface. In contrast, the C2AB domain of synaptotagmin 1 could not be detected to bind to SNARE complexes in solution (Supplemental Figure 8C). Whereas it remains formally possible that the lack of

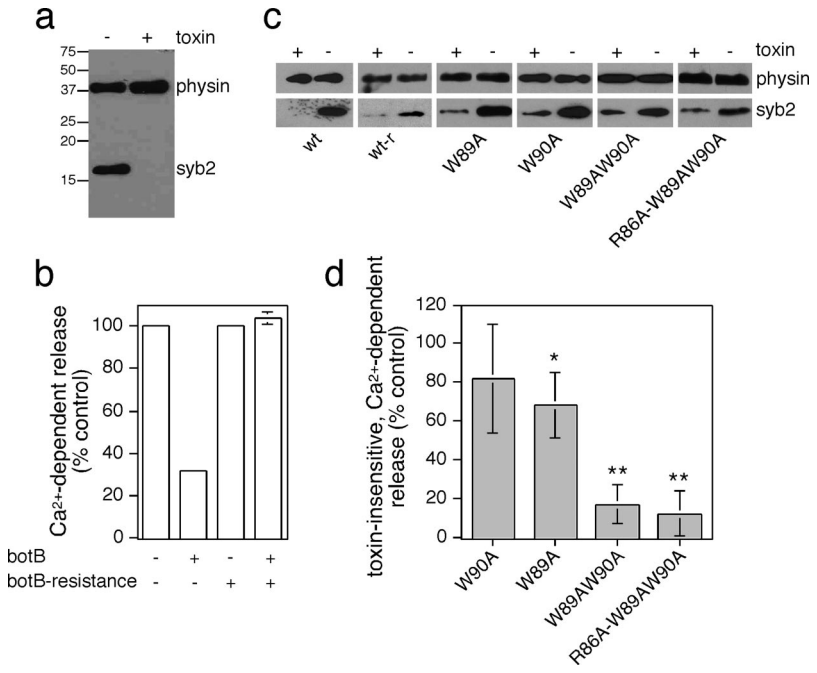

Figure 5. Toxin-insensitive, mutant syb2 is unable to rescue secretion from PC12 cells. (a) PC12 cells were permeabilized with 10 μM digitonin and incubated in the presence or absence of botB/LC, followed by detection of intact syb2 coil by Western blotting. Blots were reprobed for synaptophysin (physin) to determine equal amounts of protein loading. (b) PC12 cells, transfected with a plasmid encoding for hGH as well as wild-type or botulinum toxin-resistant syb2 (Q76V,F77W) were permeabilized with 10 μM digitonin and incubated in the presence or absence of botB/LC. Ca^{2+}-dependent hGH release was evoked by 10 μM Ca^{2+} for 10 min and compared with basal release (0 μM Ca^{2+}). The amount of hGH in the medium and in the cells was determined by an enzyme-linked immunosorbent assay, and the percentage of secreted hGH, and the total amount of hGH, were calculated against an hGH standard curve. The graph is a representative of two independent experiments with duplicate data points. Error bars are only shown if larger than bar columns. (c) Cells were transfected with wild-type or toxin-resistant wild-type syb2 (wt-r), or toxin-resistant mutant syb2 as indicated, and treated with botB/HnLC upon permeabilization to compare expression levels. (d) To standardize results from repeated experiments, secretion observed in the presence of toxin-insensitive, wild-type syb2 was set to 100%, and the relative lack of rescue of secretion of test plasmids in the presence of toxin normalized to this control. Values are means ± SEM (n = 3–5). The statistical significance of differences from wild-type were analyzed by a Student's *t* test (*$p < 0.05$; **$p < 0.01$).

synaptotagmin 1 binding is a consequence of SNARE complex dimerization, this is unlikely, because no synaptotagmin 1 binding could be detected, even on overexposed blots, in fractions migrating slightly behind the SNARE complex dimer peak and containing a minor population of SNARE complex monomers (data not shown). Such lack of comigration of soluble synaptotagmin 1 with SNARE complexes during size-exclusion chromatography has been previously observed (Bowen *et al*., 2005), indicative of a low-affinity interaction in solution. In either case, various structural and mutational data (Chen *et al*., 2002; Rickman *et al*., 2006; Lynch *et al*., 2007) further indicate that residues distinct from those involved in dimerization seem to be responsible for complexin and synaptotagmin binding to SNARE complexes.

W89 and W90 of syb2 have been implicated in binding to phospholipids (Quetglas *et al*., 2000, 2002; de Haro *et al*., 2004). In fact, it has been suggested that the reversible insertion of these residues of syb2 into the synaptic vesicle membrane may decrease the availability of syb2 and hence the probability of SNARE complex formation (Hu *et al*., 2002; Kweon *et al*., 2003). We therefore also examined SNARE complex dimers formed using a syb2 mutant in which the tryptophans were replaced with hydrophilic serine residues known to support rapid SNARE complex formation (Kweon *et al*., 2003). Expression of syb2(R86A,W89S, W90S) inhibited evoked secretion to approximately the same level as syb2(R86A,W89A,W90A) (Figure 6C). The stability of dimers formed using this mutant was virtually identical to that formed using syb2(R86A,W89A,W90A) (Figure 3C), and the stability of monomers was essentially the same as wild-type (Figure 3, D and E and Table 2B). Analogous to results obtained using the toxin rescue assay, syb2(W89A) displayed a dominant-negative effect on secretion, whereas syb2(W90A) was without effect (Figure 6D). Hence, the inhibitory effects of the mutants analyzed here are likely not due to interfering with calmodulin and/or phospholipid binding of syb2, as suggested previously (Quetglas *et al*., 2000, 2002; de Haro *et al*., 2004), but they are consistent with a mechanism involving impaired SNARE complex multimerization.

DISCUSSION

A better understanding of the mechanistic aspects of vesicle exocytosis depends on a quantitative characterization of the elements driving this process. Functional studies have clearly indicated that multiple SNARE complexes cooperate to bring about an individual vesicular fusion event (Hua and Scheller, 2001; Keller and Neale, 2001; Han *et al*., 2004; Keller *et al*., 2004; Montecucco *et al*., 2005), with the number of participating complexes possibly affecting the speed of opening, or the diameter of the fusion pore (Han *et al*., 2004). Although oligomerization may be an inherent feature of SNARE complexes, a detailed description of how such interactions take place and their relevance for membrane fusion has been lacking. In this study, we describe and characterize a defined SNARE complex dimer that forms with micromolar affinity in solution in vitro, and provide evidence for its role in neurosecretion in vivo.

The soluble part of SNARE complexes was found to form dimers with the C termini of both monomers interacting at an obtuse angle. This novel and surprising structure is quite distinct from all lattice interactions between neuronal SNARE complex monomers displayed in the crystal structure (Sutton *et al*., 1998) (PDB entry 1SFC). Although one such crystallographic dimer is formed toward the C termini of both SNARE complex monomers, with W89 of syb2 part of the interaction interface (Supplemental Figure 9), the alignment of monomers along their entire length make this "closed" crystal form distinct from the open, wing-shaped structure of dimers as identified in solution. Hydrodynamic bead modeling of this crystallographic dimer confirms that its hydrodynamic properties are very different from those observed experimentally. In addition, our biochemical and biophysical data strongly indicate the existence of a homogeneous population of dimers. Thus, interactions favored in

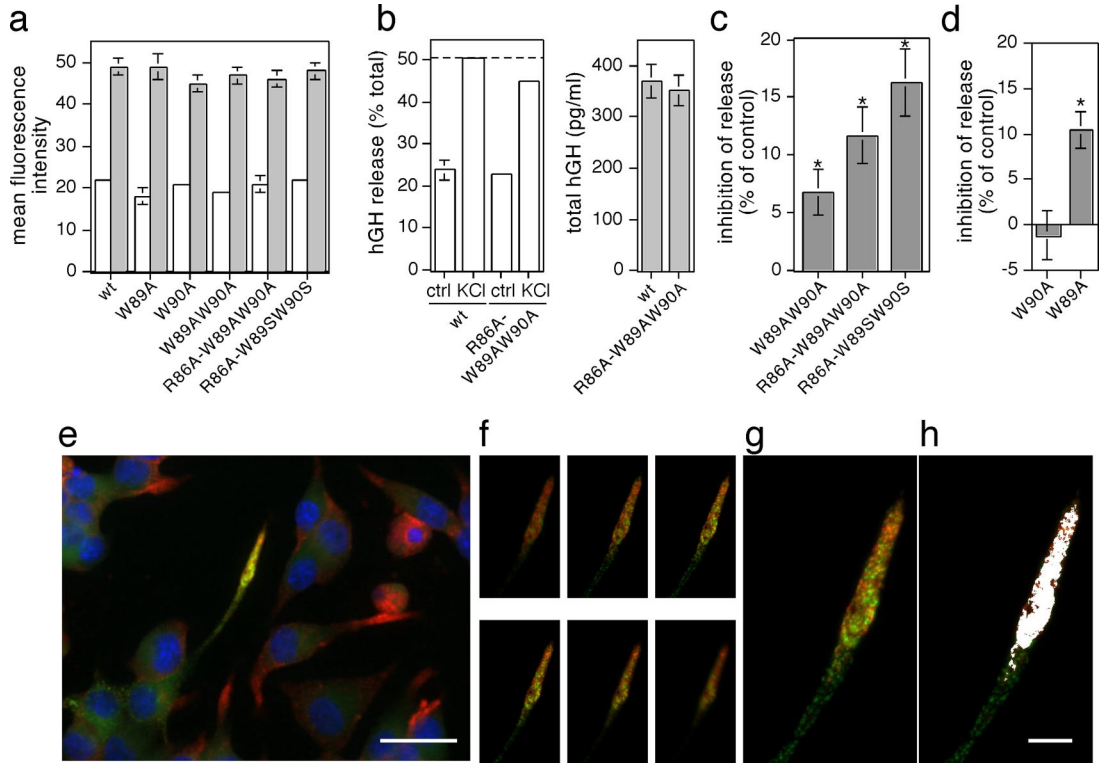

Figure 6. Syb2 mutants display dominant-negative secretory effects. (a) Expression of syb2, or syb2 mutants analyzed, relative to endogenous levels. (b) Example of hGH secretion experiment in cells transfected with wild-type or R86A-W89AW90A mutant syb2. Cells were stimulated for 5 min with physiological saline (ctrl) or high K^+ (KCl). The amount of hGH in the medium and in the cells was determined by an enzyme-linked immunosorbent assay, and the percentage of secreted hGH (left) and the total amount of hGH (right) were calculated against an hGH standard curve. Error bars are only depicted when larger than column lines. (c) To standardize results from repeated experiments, secretion observed in the presence of wild-type syb2 was set to 100%, and the relative inhibition of secretion of test plasmids normalized to control. Values are means ± SEM (n = 5–8; *$p < 0.01$). (d) Secretory effects observed with the indicated individual syb2 mutants. Analysis was done as described above. Values are means ± SEM (n = 4; *$p < 0.01$). (e) GFP-tagged, R86A-W89SW90S mutant syb2 is properly localized to neuritic appendages, as revealed by double staining with synaptotagmin (red). Bar, 20 μm. (f) Individual image acquisition (0.35-μm z-step sizes) of the appendage depicted in e. Maximum intensity projection of individual image stacks (g) and pseudocolored colocalization (white) (h). Bar, 5 μm.

crystal lattices may not be observed in other contexts (Vestergaard *et al*., 2005).

Although dimerization between cytosolic domains is likely to play an important role in the multimerization of SNARE complexes, the overall oligomeric status and shape of SNARE complexes in vivo may be further influenced by the juxtaposition of the membrane, the presence of the transmembrane domains, and accessory factors. Indeed, previous studies have shown that native SNARE complexes purified from brain, or SNARE complexes assembled from recombinant full-length SNAREs containing transmembrane domains, assemble into star-shaped particles mostly containing three or four bundles emanating from their center (Rickman *et al*., 2005). Such structure may be obtained when two dimers associate with each other through their transmembrane domains (Hohl *et al*., 1998; Laage *et al*., 2000; Bowen *et al*., 2002; Roy *et al*., 2004). Unfortunately, when only one of the two SNAREs carried a transmembrane domain, reassembly experiments led to the generation of large irregular aggregates (Rickman *et al*., 2005). This makes it difficult to determine the exact contributions of the transmembrane domains and/or membrane-proximal regions of syb2 to the formation of oligomeric structures obtained with full-length SNAREs. Similarly, the need for detergent solubilization precludes analysis of whether identified SNARE complex multimers are present in their *trans*- or *cis*-forms, and additional evidence for the existence and importance of SNARE complex oligomers may be best obtained using in vivo approaches.

Earlier studies using syb2(W89A,W90A) had suggested that these residues mediate the binding of syb2 to calmodulin (Quetglas *et al*., 2002; de Haro *et al*., 2004). However, no single mutational analysis was performed to corroborate these results. The consensus motif for Ca^{2+}-dependent calmodulin binding involves select hydrophobic residues at positions 1-5-8-14, and an overall net electrostatic charge of +2 to +6 (Rhoads and Friedberg, 1997). As such, W90 is at position 14 of this motif, and a mutation to alanine at this position would not be tolerated (Rhoads and Friedberg, 1997). We find that syb2(W90A) has no effect on secretion either in the presence or absence of endogenous syb2. Similarly, the overall net charge of the calmodulin binding motif within syb2 is +3, and the secretory effect of another mutant (syb2(K83A,K87V)) was suggested to be due to eliminating those charge requirements (Quetglas *et al*., 2002). However, because K83 is part of the SNARE motif, the effects of this mutant may have been due to altered SNARE complex stability, which was not assessed in sufficient detail. Finally, mutating W89 and W90 to hydrophilic serines does not enhance secretion, as would be expected if the availability of syb2 would be restricted due to its interacting with the hydrophobic part of the phospholipid bilayer (Kweon *et al*.,

2003). Our analysis shows that the ability of syb2 mutants to reduce SNARE complex dimer stability in vitro parallels their inhibition of secretion in vivo. Thus, although we cannot fully exclude compound effects, our data indicate that the secretory effects observed with the syb2 mutants are most likely due to interfering with SNARE complex dimer stability in vivo.

The dimerization of neuronal SNARE complexes may generate an important intermediate during evoked secretion. This intermediate may be transient in vivo, formed after *trans*-SNARE complex assembly and close to the point of fusion. Although detailed electrophysiological experiments will be needed to determine the precise role of SNARE complex dimers in membrane fusion events, one can speculate from their solution structure how they might contribute toward formation of an oligomeric complex around a fusion pore, consistent with the energies required to bring about membrane fusion (Li *et al*., 2007). It is interesting to note that the syb2(W89A,W90A) mutant does not seem to be defective in mediating liposomal fusion events (Siddiqui *et al*., 2007), whereas it profoundly inhibits Ca^{2+}-dependent secretion. Thus, secretory defects using the syb2 dimerization mutants only seem to be evident in cell systems requiring cooperativity between SNARE complexes. Such SNARE complex dimerization may improve the efficiency of vesicle exocytosis by contributing to the cooperative relationship between calcium and synaptic transmission.

ACKNOWLEDGMENTS

We thank J. Zimmerberg, R. Fernandez-Chacón, and D. Thornton for critical comments. We thank S. High (University of Manchester) for the full-length syb2 construct, G. Schiavo (Cancer Research UK) for the SNAP-25 construct, M. Carrington (University of Cambridge) for the Venus construct, H. McMahon (University of Cambridge) for the complexin constructs, A. F. Parlow (National Hormone and Pituitary Program, NIDDK) for the anti-hGH antibody, and the European Synchrotron Radiation Facility (ESRF) and T. Narayanan (ESRF) for assistance with SAXS measurements. This work was supported by the UK Medical Research Council grants G9722026 and G9901377 and Spanish Ministerio de Educación y Ciencia (MEC) grants BFU2004-02969 and BFU2007-63635). The laboratory of S. H. is member of the Network for Cooperative Research on Membrane Transport Proteins, cofunded by the MEC and the European Regional Development Fund BFU2007-30688-E/BFI). S. H. is supported by a Ramón y Cajal Fellowship. E. F. is supported by a fellowship (FPI) from the Spanish MEC.

REFERENCES

Antonin, W., Holroyd, C., Fasshauer, D., Pabst, S., Fischer von Mollard, G., and Jahn, R. (2000). A SNARE complex mediating fusion of late endosomes defines conserved properties of SNARE structure and function. EMBO J. *19*, 6453–6464.

Bevan, S., and Wendon, L. M. (1984). A study of the action of tetanus toxin at rat soleus neuromuscular junctions. J. Physiol. *348*, 1–17.

Bowen, M. E., Engelman, D. M., and Brunger, A. T. (2002). Mutational analysis of synaptobrevin transmembrane domain oligomerization. Biochemistry *41*, 15861–15866.

Bowen, M. E., Weninger, K., Ernst, J., Chu, S., and Brunger, A. T. (2005). Single-molecule studies of synaptotagmin and complexin binding to the SNARE complex. Biophys. J. *89*, 690–702.

Chen, X., Tomchick, D. R., Kovrigin, E., Arac, D., Machius, M., Südhof, T. C., and Rizo, J. (2002). Three-dimensional structure of the complexin/SNARE complex. Neuron *33*, 397–409.

Chilcote, T. J., Galli, T., Mundigl, O., Edelmann, L., McPherson, P. S., Takei, K., and De Camilli, P. (1995). Cellubrevin and synaptobrevins: similar subcellular localization and biochemical properties in PC12 cells. J. Cell Biol. *129*, 219–231.

Chin, D., and Means, A. R. (2000). Calmodulin: a prototypical calcium sensor. Trends Cell Biol. *10*, 322.

Cull-Candy, S. G., Lundh, H., and Thesleff, S. (1976). Effects of botulinum toxin on neuromuscular transmission in the rat. J. Physiol. *260*, 177–203.

de Haro, L., Ferracci, G., Opi, S., Iborra, C., Quetglas, S., Miquelis, R., Leveque, C., and Seagar, M. (2004). Ca^{2+}/calmodulin transfers the membrane-proximal lipid-binding domain of the v-SNARE synaptobrevin from cis to trans bilayers. Proc. Natl. Acad. Sci. USA *101*, 1578–1583.

Ernst, J. A., and Brünger, A. T. (2003). High resolution structure, stability, and synaptotagmin binding of a truncated neuronal SNARE complex. J. Biol. Chem. *278*, 8630–8636.

Fasshauer, D., Eliason, W. K., Brünger, A. T., and Jahn, R. (1998). Identification of a minimal core of the synaptic SNARE complex sufficient for reversible assembly and disassembly. Biochemistry *37*, 10354–10362.

Fasshauer, D., Otto, H., Eliason, W. K., Jahn, R., and Brünger, A. T. (1997). Structural changes are associated with soluble N-ethylmaleimide-sensitive fusion protein attachment protein receptor complex formation. J. Biol. Chem. *272*, 28036–28041.

Fiebig, K. M., Rice, L. M., Pollock, E., and Brünger, A. T. (1999). Folding intermediates of SNARE complex assembly. Nat. Struct. Biol. *6*, 117–123.

Giraudo, C. G., Eng, W. S., Melia, T. J., and Rothman, J. E. (2006). A clamping mechanism involved in SNARE-dependent exocytosis. Science *313*, 676–680.

Han, X., Wang, C. T., Bai, J., Chapman, E. R., and Jackson, M. B. (2004). Transmembrane segments of syntaxin line the fusion pore of Ca^{2+}-triggered exocytosis. Science *304*, 289–292.

Hanson, P. I., Roth, R., Morisaki, R., Jahn, R., and Heuser, J. E. (1997). Structure and conformational changes in NSF and its membrane receptor complexes visualized by quick-freeze/deep-etch electron microscopy. Cell *90*, 523–536.

Hohl, T. M., Parlati, F., Wimmer, C., Rothman, J. E., Söllner, T. H., and Engelhardt, H. (1998). Arrangement of subunits in 20S particles consisting of NSF, SNAPs, and SNARE complexes. Mol. Cell *2*, 539–548.

Hu, C., Ahmed, M., Melia, T. J., Söllner, T., Mayer, T., and Rothman, J. E. (2003). Fusion of cells by flipped SNAREs. Science *300*, 1745–1749.

Hu, K., Carroll, J., Fedorovich, S., Rickman, C., Sukhodub, A., and Davletov, B. (2002). Vesicular restriction of synaptobrevin suggests a role for calcium in membrane fusion. Nature *415*, 646–650.

Hua, Y., and Scheller, R. H. (2001). Three SNARE complexes cooperate to mediate membrane fusion. Proc. Natl. Acad. Sci. USA *98*, 8065–8070.

Jahn, R., and Scheller, R. H. (2006). SNAREs-engines for membrane fusion. Nat. Rev. Mol. Cell Biol. *7*, 631–643.

Keller, J. E., Cai, F., and Neale, E. A. (2004). Uptake of botulinum neurotoxin into cultured neurons. Biochemistry *43*, 526–532.

Keller, J. E., and Neale, E. A. (2001). The role of the synaptic protein SNAP-25 in the potency of botulinum neurotoxin type A. J. Biol. Chem. *276*, 13476–13482.

Kweon, D. H., Chen, Y., Zhang, F., Poirier, M., Kim, C. S., and Shin, Y. K. (2002). Probing domain swapping for the neuronal SNARE complex with electron paramagnetic resonance. Biochemistry *41*, 5449–5452.

Kweon, D.-H., Kim, C. S., and Shin, Y.-K. (2003). Regulation of neuronal SNARE assembly by the membrane. Nat. Struct. Biol. *10*, 440–447.

Laage, R., Rohde, J., Brosig, B., and Langosch, D. (2000). A conserved membrane-spanning amino acid motif drives homomeric and supports heteromeric assembly of presynaptic SNARE proteins. J. Biol. Chem. *275*, 17481–17487.

Li, F., Pincet, F., Perez, E., Eng, W. S., Melia, T. J., Rothman, J. E., and Tareste, D. (2007). Energetics and dynamics of SNAREpin folding across lipid bilayers. Nat. Struct. Mol. Biol. *14*, 890–896.

Littleton, J. T., Bai, J., Vyas, B., Desai, R., Baltus, A. E., Garment, M. B., Carlson, S. D., Ganetzky, B., and Chapman, E. R. (2001). Synaptotagmin mutants reveal essential functions for the C2B domain in Ca^{2+}-triggered fusion and recycling of synaptic vesicles in vivo. J. Neurosci. *21*, 1421–1433.

Lynch, K. L., Gerona, R.R.L., Larsen, E. C., Marcia, R. F., Mitchell, J. C., and Martin, T.F.J. (2007). Synaptotagmin C2A loop 2 mediates Ca^{2+}-dependent SNARE interactions essential for Ca^{2+}-triggered vesicle exocytosis. Mol. Biol. Cell *18*, 4957–4968.

Margittai, M., Fasshauer, D., Pabst, S., Jahn, R., and Langen, R. (2001). Homo- and heterooligomeric SNARE complexes studied by site-directed spin labeling. J. Biol. Chem. *276*, 13169–13177.

Montecucco, C., Schiavo, G., and Pantano, S. (2005). SNARE complexes and neuroexocytosis: how many, how close? Trends Biochem. Sci. *30*, 367.

Pobbati, A. V., Stein, A., and Fasshauer, D. (2006). N- to C-terminal SNARE complex assembly promotes rapid membrane fusion. Science *313*, 673–676.

Quetglas, S., Iborra, C., Sasakawa, N., De Haro, L., Kumakura, K., Sato, K., Leveque, C., and Seagar, M. (2002). Calmodulin and lipid binding to synaptobrevin regulates calcium-dependent exocytosis. EMBO J. *21*, 3970–3979.

Quetglas, S., Leveque, C., Miquelis, R., Sato, K., and Seagar, M. (2000). Ca^{2+}-dependent regulation of synaptic SNARE complex assembly via a calmodulin- and phospholipid-binding domain of synaptobrevin. Proc. Natl. Acad. Sci. USA *97*, 9695–9700.

Rhoads, A. R., and Friedberg, F. (1997). Sequence motifs for calmodulin recognition. FASEB J. *11*, 331–340.

Rickman, C., Hu, K., Carroll, J., and Davletov, B. (2005). Self-assembly of SNARE fusion proteins into star-shaped oligomers. Biochem. J. *388*, 75–79.

Rickman, C., Jiménez, J. L., Graham, M. E., Archer, D. A., Soloviev, M., Burgoyne, R. D. and Davletov, B. (2006). Conserved prefusion protein assembly in regulated exocytosis. Mol. Biol. Cell *17*, 283–294.

Rizo, J., Chen, X., and Arac, D. (2006). Unraveling the mechanisms of synaptotagmin and SNARE function in neurotransmitter release. Trends Cell Biol. *16*, 339.

Roy, R., Laage, R., and Langosch, D. (2004). Synaptobrevin transmembrane domain dimerization-revisited. Biochemistry *43*, 4964–4970.

Siddiqui, T. J., Vites, O., Stein, A., Heintzmann, R., Jahn, R., and Fasshauer, D. (2007). Determinants of synaptobrevin regulation in membranes. Mol. Biol. Cell *18*, 2037–2046.

Sorensen, J. B., Wiederhold, K., Muller, E. M., Milosevic, I., Nagy, G., de Groot, B. L., Grubmuller, H., and Fasshauer, D. (2006). Sequential N- to C-terminal SNARE complex assembly drives priming and fusion of secretory vesicles. EMBO J. *25*, 955–966.

Spotorno, B., Piccinini, L., Tassara, G., Ruggiero, C., Nardini, M., Molina, F., and Rocco, M. (1997). BEAMS (BEAds Modelling System): a set of computer programs for the generation, the visualization and the computation of the hydrodynamic and conformational properties of bead models of proteins. Eur. Biophys. J. *25*, 373–384.

Stewart, B. A., Mohtashami, M., Trimble, W. S., and Boulianne, G. L. (2000). SNARE proteins contribute to calcium cooperativity of synaptic transmission. Proc. Natl. Acad. Sci. USA *97*, 13955–13960.

Südhof, T. C. (2004). The synaptic vesicle cycle. Annu. Rev. Neurosci. *27*, 509–547.

Sugita, S., Janz, R., and Südhof, T. C. (1999). Synaptogyrins regulate Ca^{2+}-dependent exocytosis in PC12 cells. J. Biol. Chem. *274*, 18893–18901.

Sutton, J. M., Wayne, J., Scott-Tucker, A., O'Brien, S. M., Marks, P. M., Alexander, F. C., Shone, C. C., and Chaddock, J. A. (2005). Preparation of specifically activatable endopeptidase derivatives of *Clostridium botulinum* toxins type A, B, and C and their applications. Protein Expr. Purif. *40*, 31–41.

Sutton, R. B., Fasshauer, D., Jahn, R., and Brünger, A. T. (1998). Crystal structure of a SNARE complex involved in synaptic exocytosis at 2.4Å resolution. Nature *395*, 347–353.

Svergun, D. I. (1999). Restoring low resolution structure of biological macromolecules from solution scattering using simulated annealing. Biophys. J. *76*, 2879–2886.

Svergun, D. I., Petoukhov, M. V., and Koch, M. H. (2001). Determination of domain structure of proteins from X-ray solution scattering. Biophys. J. *80*, 2946–2953.

Söllner, T., Bennett, M. K., Whiteheart, S. W., Scheller, R. H., and Rothman, J. E. (1993). A protein assembly-disassembly pathway in vitro that may correspond to sequential steps of synaptic vesicle docking, activation, and fusion. Cell *75*, 409–418.

Tang, J., Maximov, A., Shin, O., Dai, H., Rizo, J., and Südhof, T. C. (2006). A complexin/synaptotagmin 1 switch controls fast synaptic vesicle exocytosis. Cell *126*, 1175–1187.

Tokumaru, H., Umayahara, K., Pellegrini, L., Ishizuka, T., Saisu, H., Betz, H., Augustine, G., and Abe, T. (2001). SNARE complex oligomerization by synaphin/complexin is essential for synaptic vesicle exocytosis. Cell *104*, 421–432.

Vestergaard, B., Sanyal, S., Roessle, M., Mora, L., Buckingham, R. H., Kastrup, J. S., Gajhede, M., Svergun, D. I., and Ehrenberg, M. (2005). The SAXS solution structure of RF1 differs from its crystal structure and is similar to its ribosome bound cryo-EM structure. Mol. Cell *20*, 929–938.

Weber, T., Zemelman, B. V., McNew, J. A., Westermann, B., Gmachl, M., Parlati, F., Söllner, T. H., and Rothman, J. E. (1998). SNAREpins: minimal machinery for membrane fusion. Cell *92*, 759–772.

Wojcik, S. M., and Brose, N. (2007). Regulation of membrane fusion in synaptic excitation-secretion coupling: speed and accuracy matter. Neuron *55*, 11–24.